Supporting Information

Cobalt doped Mo_5N_6 as a noble-metal-free novel cocatalyst for promoting photocatalytic hydrogen production of g-C_3N_4 nanosheets

Pengyuan Qiu[a], Ruhao Hu[a], Xinyu Wang[a], Yanjun Xue[a], Jian Tian[, a], Xiaobo Chen[*, b]*

[a] School of Materials Science and Engineering, Shandong University of Science and Technology, Qingdao 266590, China

[b] Department of Chemistry, University of Missouri, Kansas City, MO 64110, USA

[*] Corresponding authors. E-mail addresses: jiantian@sdust.edu.cn (J. Tian), chenxiaobo@umkc.edu (X. Chen)

Characterization

The XRD patterns were carried out by a Bruker D8 Advance powder X-ray diffractometer. The surface characteristic of samples was measured on a scanning electron microscope (FEI Nova Nanosem 450). The crystal structure and morphology of samples were measured by a high-resolution transmission electron microscope (HR-TEM) (FEI Tecnai F30). The XPS was measured on a Thermo ESCALAB 250XI instrument. The UV–Vis DRS spectra were measured by a Hitachi UV-2550 UV–Vis spectrophotometer.

Photoelectrochemical measurements

The photocurrent response and electrochemical impedance of samples were measured via an electrochemical workstation (Shanghai Chenhua CHI660D) in a three-

electrode system, in which the sample electrode is used as the photocathode, Ag/AgCl as the reference electrode, a Pt wire as the counter electrode, 0.5 M Na_2SO_4 aqueous solution as the electrolyte. The working electrodes were prepared as follows: 25 mg photocatalysts and 1 mg ethyl cellulose were dispersed into a solution containing 0.5 mL terpineol and 0.5 mL ethanol by 25 min sonication to prepare a homogeneous slurry. Then, 0.4 mL of the slurry was dropped onto the pretreated stannic oxide (FTO) conductive glass with an exposed area of 4.0 cm^2 (2 cm×2 cm). The 500 W Xe arc lamp equipped with an AM-1.5 filter was adopted as the light source. For EIS measurement, the amplitude of the measurement was 5 mV and the frequency range of the measurement was 10^{-2}~10^5 H_Z. For Mott-Schottky plot measurement, the amplitude of the measurement is 5 mV and the frequency of the measurement was 1000 H_Z.

Photocatalytic H_2 evolution

Photocatalytic H_2 production experiments were carried out in an outer irradiation type photoreactor (100 mL quartz glass) in an N_2 environment. 25 mg sample was dispersed with a mechanical stirring in a 100 mL aqueous solution containing 20 vol % triethanolamine further photocatalytic H_2 production experiment. Before irradiation, the photocatalytic system was thoroughly degassed to remove air by bubbling N_2 for 20 min. The irradiation light source used in this study was a 300 W Xe arc lamp (CELHXF300, Beijing China Education Au-light Co., Ltd.), which is equipped with an AM-1.5 filter. The evolved gas was analyzed by a gas chromatograph (Techcomp GC-7920) equipped with a thermal conductivity detector (TCD). The apparent quantum

efficiency (AQE) was measured under Ultraviolet light (λ=370 nm). The apparent quantum efficiency (AQE) was tested and calculated according to the equation:

$$AQE = \frac{\text{nmuber of reacted electrons}}{\text{number of incident photons}} \times 100 = \frac{\text{number of evolved } H_2 \text{ molecules} \times 2}{\text{number of incident photons}} \times 100\% \quad (1)$$

Density functional theory (DFT) calculations

We have employed the first-principles to perform all spin-polarization density functional theory (DFT) calculations within the generalized gradient approximation (GGA) using the Perdew-Burke-Ernzerhof (PBE) formulation. We have chosen the projected augmented wave (PAW) potentials to describe the ionic cores and take valence electrons into account using a plane wave basis set with a kinetic energy cutoff of 450 eV. Partial occupancies of the Kohn−Sham orbitals were allowed using the Gaussian smearing method and a width of 0.05 eV. The electronic energy was considered self-consistent when the energy change was smaller than 10^{-5} eV. The Brillouin zone integral uses the surfaces structures of 2×2×1 monkhorst pack K point sampling for surface structures. A geometry optimization was considered convergent when the energy change was smaller than 0.05 eV $Å^{-1}$. Finally, the adsorption energies(E_{ads}) were calculated as:

$$E_{ads}=E_{ad/sub}-E_{ad}-E_{sub} \quad (2)$$

where $E_{ad/sub}$, E_{ad}, and E_{sub} are the total energies of the optimized adsorbate/substrate system, the adsorbate in the gas phase, and the clean substrate, respectively. The free energy (ΔG) for elemental reaction step was calculated as:

$$\Delta G=\Delta E+\Delta E_{ZPE}-T\Delta S \quad (3)$$

where ΔE is the difference between the total energy, ΔE_{ZPE} and ΔS are the differences in the zero-point energy and the change of entropy, T is the temperature (T =300 K in this work), respectively.

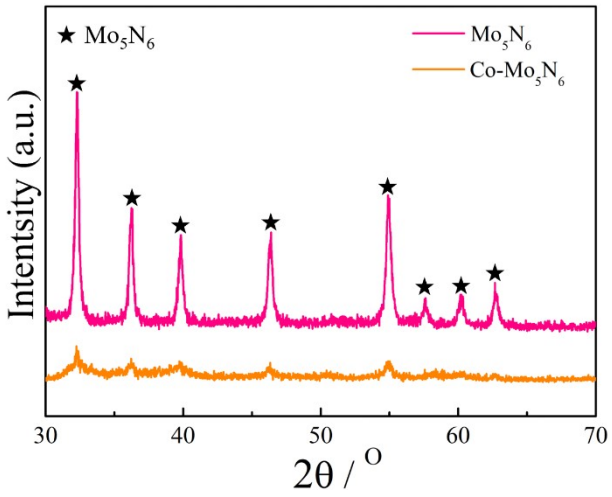

Figure S1. XRD patterns of Mo_5N_6 and Co-Mo_5N_6.

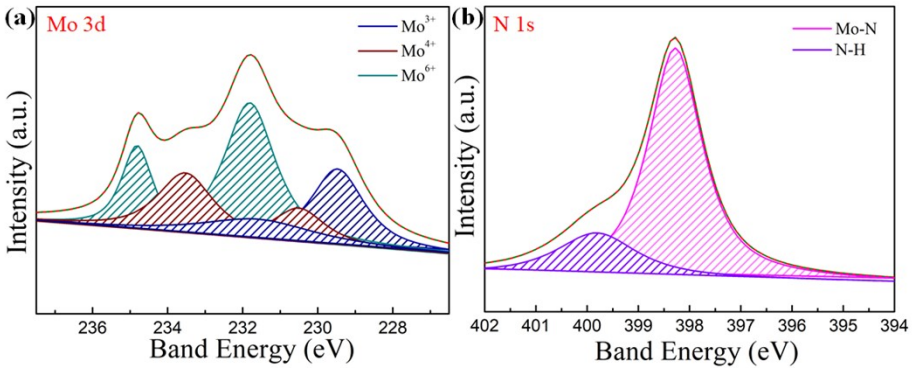

Figure S2. XPS spectra of Mo_5N_6:(a) Mo 3d and (b) N 1s.

Table S1. Element content table of Co-Mo_5N_6/g-C_3N_4 hybrids.

Element	**`Weight percentage (100%)**
C	45.94
N	51.4

Mo	1.18
Co	1.48

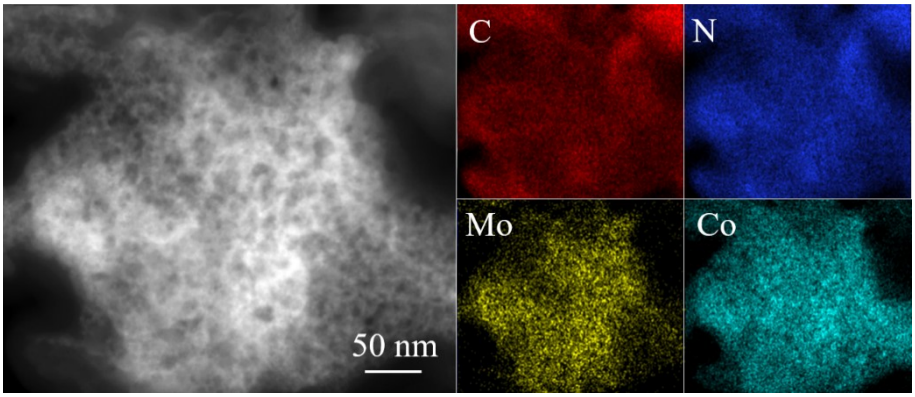

Figure S3. TEM-EDX element mapping of Co-Mo_5N_6/g-C_3N_4 hybrids.

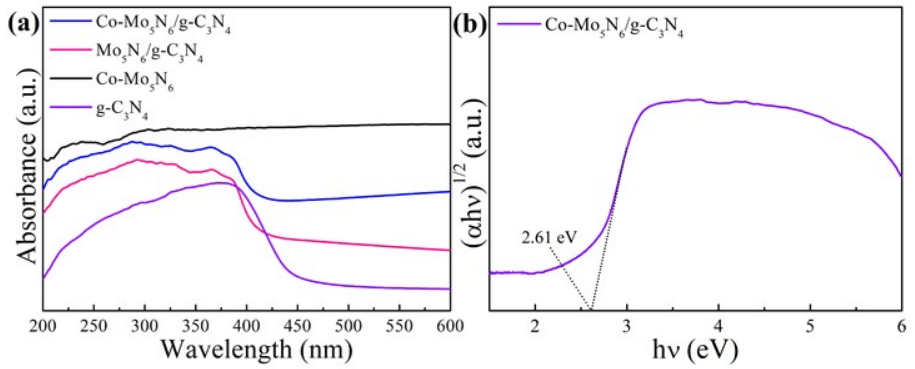

Figure S4. (a) UV–Vis light absorption of all samples and (b) band gap values spectra of pure g-C_3N_4 NSs.

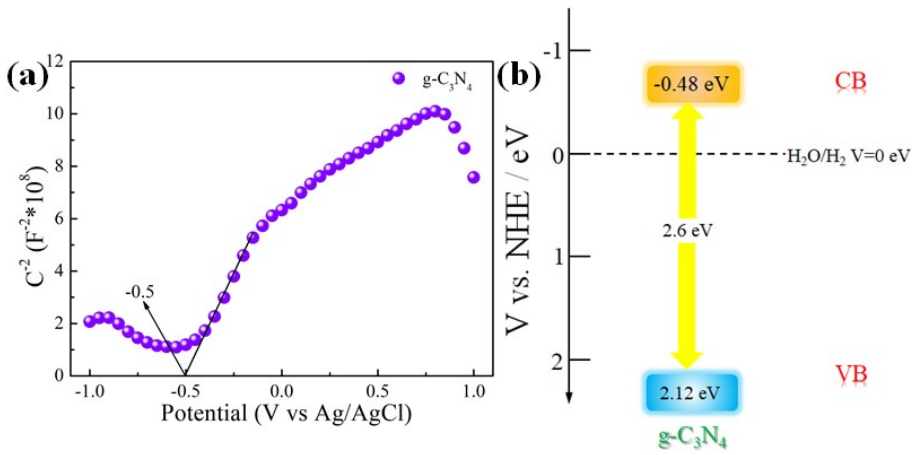

Figure S5. (a) Mott-Schottky plots and (b) schematic diagram of the band gap of pure g-C_3N_4 NSs.

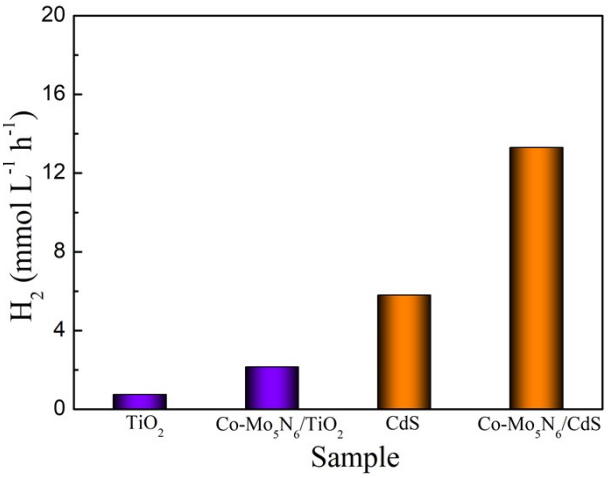

Figure S6. Photocatalytic H_2 production rates of TiO_2, Co-Mo_5N_6/TiO_2, CdS and Co-Mo_5N_6/CdS.

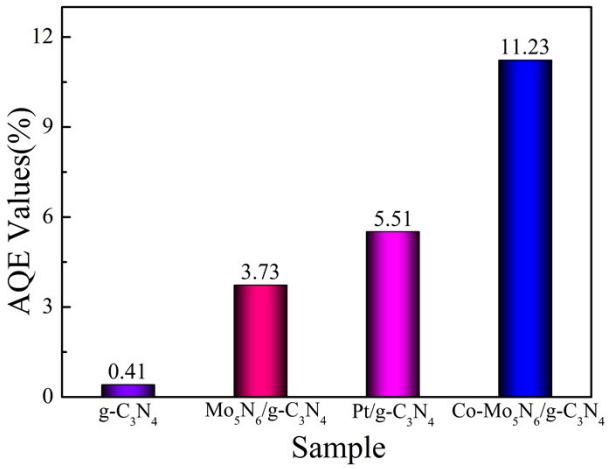

Figure S7. AQE values under light at λ=370 nm of pure g-C_3N_4 NSs, Mo_5N_6/g-C_3N_4 and Co-Mo_5N_6/g-C_3N_4 hybrids.

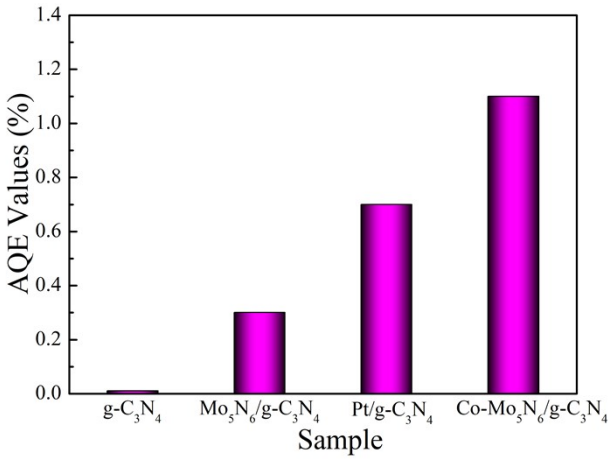

Figure S8. AQE values under light at λ=456 nm of pure g-C_3N_4 NSs, Mo_5N_6/g-C_3N_4, Pt/g-C_3N_4, and Co-Mo_5N_6/g-C_3N_4 hybrids.

Table S2. The summary of photocatalytic H_2 production activity of the photocatalysts.

Photocatalysts	**Photocatalytic H_2 production activity**	**Refs.**
Co@g-C_3N_4	2481 μmol h^{-1} g^{-1} (50 mg, 10 vol% TEOA, 3 wt % Pt)	1
0.6 % Bi_2S_3/g-C_3N_4	3394.1 μmol g^{-1} h^{-1} (30 mg, 0.35 M of Na_2S, 0.25 M of Na_2SO_3)	2
B-CNNT/CoP-2.45%	784 μmol h^{-1} g^{-1} (50 mg, 10 vol% TEOA)	3
CN/Sn_3O_4-3	1961.4 μmol g^{-1} h^{-1} (50 mg, 10 vol% TEOA)	4
3Ru-15Ti_3AlC_2/g-C_3N_4	1445 μmol L^{-1} h^{-1} g^{-1} (100 mg, 100 mL solution of 5% methanol-water)	5
BPNS/CdS	57.64 μmol L^{-1} h^{-1} (60 mg, N_2, 250 mL H_2O of 1 vol % methanol)	6
Co-Mo_5N_6/g-C_3N_4	3690.37μmol g^{-1} h^{-1} (20 mg, 100 mL H_2O of 20 vol % TEOA)	This work

[1] W. Zhang, Y. Fu, Q. Peng, Q. Yao, X. Wang, A. Yu, Z. Chen, Chem. Eng. J. 394 (2020) 124822.
[2] B. Zhang, H. Shi, Y. Yan, C. Liu, X. Hu, E. Liu, J. Fan, Colloid. Surface A. 608 (2021) 125598.
[3] Y. Jiao, Y. Li, J. Wang, Z. He, Z. Li, J. Colloid Interface Sci. 595 (2021) 69-77.
[4] Y. Zhu, Y. Cui, B. Xiao, J. Ou-yang, H. Li, Z. Chen, Mater. Sci. Semicond. Process. 129 (2021) 105767.
[5] B. Tahir, M. Tahir, Mater. Res. Bull. 144 (2021) 111493.
[6] Z. Shen, Y. Yuan, P. Wang, W. Bai, L. Pei, S. Wu, Z. Yu, Z. Zou, ACS Appl. Mater. Interfaces 12.15 (2020) 17343-17352.